PNAS
www.pnas.org

SUPPLEMENTAL INFORMATION FOR

Upregulation of the manganese transporter SLC30A10 by hypoxia inducible factors defines a homeostatic response to manganese toxicity

Chunyi Liu [1], Thomas Jursa [2], Michael Aschner [3], Donald R. Smith [2], and Somshuvra Mukhopadhyay [1, *]

[1] Division of Pharmacology & Toxicology, College of Pharmacy; and Institute for Neuroscience, The University of Texas at Austin, Austin TX 78712. [2] Department of Microbiology and Environmental Toxicology, University of California, Santa Cruz, CA 95064. [3] Department of Molecular Pharmacology, Albert Einstein College of Medicine, Bronx, New York 10461.

[*] Corresponding author: Somshuvra Mukhopadhyay, Associate Professor, Division of Pharmacology & Toxicology, The University of Texas at Austin, 3.510E BME, 107 W. Dean Keeton, Austin, TX 78712. E-mail: som@austin.utexas.edu

This PDF file includes:

Extended Methods

Animal experiments. All experiments with mice were approved by the Institutional Animal Care and Use Committee of the University of Texas at Austin.

We used a well-characterized drinking water-based Mn exposure regimen to model human environmental Mn exposure by providing mice with ~50 mg $MnCl_2.4H_2O$/kg body weight daily (~15 mg absolute Mn/kg per day) from birth until 8 weeks of age. This, and related similar, dosing regimens: 1) approximate the increase in Mn exposure in humans consuming well water contaminated with 1.5 mg Mn/L, which is the median well water concentration associated with neurological deficits in children; 2) increase brain Mn levels by ~2-3 fold, similar to human patients; 3) produce measurable neurobehavioral deficits without overt toxicity; and 4) model exposure to Mn in developmentally-sensitive early-life and adolescent periods (1). Pre-weaning Mn was delivered by pipette directly into the mouth, and post-weaning Mn was delivered in drinking water using procedures described in detail in our ref. (1). In brief, pre-weaning dosing was adjusted to each animal's body weight. For this, a stock solution of 69.2 mg absolute Mn/ml prepared in milliQ water was diluted in milliQ water containing 2.5% (wt/vol) of the natural sweetener Stevia (to facilitate intake by pups), and the required Mn amount (0.2 µl Mn stock/g body weight) was delivered in a dose of ~5-10 µl/animal. For post-weaning exposure, a 27.7 mg absolute Mn/ml stock solution was prepared in water and diluted to 0.069 mg absolute Mn/ml in drinking water, which provided mice with ~15 mg absolute Mn/kg per day based on a daily water intake of ~2-5 ml/mouse depending on age.

To assay for the protective effect of roxadustat, animals were exposed to roxadustat or vehicle with or without Mn in drinking water from ~4 weeks of age. Treatment lasted for 4 weeks from initiation. Roxadustat (Selleckchem) was prepared as a 50 mg/ml stock solution in DMSO, then diluted to 1 mg/ml in sterile phosphate buffered saline (PBS), and delivered by daily i.p. injection at 10 mg/kg. Vehicle was 2% DMSO in PBS. For this experiment, drinking water Mn levels were adjusted to 0.138 mg absolute Mn/ml so that animals received ~30 mg absolute Mn/kg daily. A higher level of Mn was used because exposure was initiated after weaning, which was necessary because daily i.p. injections for roxadustat delivery were not possible in the pre-weaning period.

For the Mn exposure experiment initiated at birth, breeders for C57BL/6J and 129S4/SvJaeJ mice were obtained from The Jackson Labs. Mice were crossed and litters housed in the conventional facility of the University of Texas at Austin in a room maintained at 21°C with a 12-h light-dark cycle (lights on between 7 p.m. and 7 a.m.). Animals were weaned at PND 21. After weaning, 3-4 littermates of the same sex were kept per cage. For the roxadustat protection assay, ~3-week old C57BL/6J mice were obtained from The Jackson Labs, housed in our conventional facility, and used for experiments from ~4-weeks of age. All animals were fed standard rodent chow with ~160 µg Mn/g chow (Prolab RMH 1800; LabDiet #5LL2). Animals on standard chow and drinking water not supplemented with elevated Mn have basal ganglia Mn levels that are comparable to humans (reviewed in (1)), providing a suitable baseline for the environmentally-relevant, drinking water-based Mn exposure studies performed here. We did not use chow with very high Mn levels as an exposure model (2, 3) because oral Mn exposure in humans occurs from drinking water, and human body Mn levels and neurotoxicity are associated with elevated Mn concentrations in drinking water, but not food (1, 4). Animals had free access to chow and water for the duration of the study.

Animals were euthanized using carbon dioxide and tissue dissected for qRT-PCR or ICP-MS analyses as described by us previously (5). For all analyses using brain and intestine tissue, respectively, a part of the midbrain containing the basal ganglia, and a section of the proximal small intestine ~0.5 – 1 cm distal to the stomach were used.

Cell culture. HepG2 cells were grown in Eagle's modified essential medium (MEM; Corning) with 10% fetal bovine serum (Atlanta Biologicals), 100 IU/ml penicillin (Corning), and 100 µg/ml streptomycin (Corning). 293T cells were maintained in Dulbecco's modified essential medium/F12 (Thermo) supplemented with 10% fetal bovine serum, penicillin (100 IU/ml), and streptomycin (100 µg/ml). Human primary hepatocytes were purchased from XenoTech (catalog # HPCH10+) and cultured according to protocols provided by the supplier.

Mn and drug treatments in cell culture. Cells were treated with indicated levels of Mn as $MnCl_2.4H_2O$ (Fisher). Vehicle for Mn treatment was water. Prolyl hydroxylase inhibitors roxadustat (Caymen), vadadustat, and molidustat (both APE-Bio); the HIFα inhibitor LW6 (Selleckchem); the proteasomal inhibitor MG132 (Sigma); and the transcription inhibitor actinomycin D (Sigma) were dissolved in DMSO. LW6, MG132, and actinomycin D were used at an effective concentration of 10 µM, 10 µM, and 5 µM, respectively (6, 7) while prolyl hydroxylase inhibitors were used at concentrations indicated in the figure legends. Vehicle treatment for all drugs was DMSO.

Plasmids and shRNAs. Lentivirus infections were used to stably express luciferase or dominant negative constructs, and shRNAs targeting HIF1α, HIF2α, or HIF1β/ARNT.

A luciferase reporter plasmid containing the proximal promoter of human *SLC30A10* has been previously described and was a gift of Dr. Ruth Valentine (8). The promoter fragment corresponding to bases -679 to +211 relative to the start of transcription was sub-cloned into the Xho1 and SpeI sites of pRRLSIN.cPPTLuciferase.WPRE vector (Addgene, #69251), which is a luciferase vector for lentivirus infections. Deletion mutants were generated using the loop-out modification of the QuikChange protocol.

Plasmids encoding dominant negative versions of C/EBPB, which contains an N-terminal acidic extension fused to the HLH-ZIP region, c-Jun encoding amino acid residues 123-331, and P53 encoding a truncated protein of amino acids 300-393 were obtained from Addgene (#33363, 40350, and 25989 respectively). Plasmids encoding full-length RXRα or YY1 were obtained from DNASU (#HsCD00079702 or #HsCD00005306, respectively), and dominant negative versions generated by deleting the transactivation domain (amino acids 444-462) of RXRα (9) or introducing the S339/S342 mutation in YY1 (10). Plasmids encoding VHL insensitive mouse HIF1α and HIF2α were a gift of Dr. Sadeesh Ramakrishnan (University of Pittsburgh). These open reading frames were sub-cloned into the Nhe1/EcoR1 sites of the lentivirus transfer plasmid LAMP1-mRFP-FLAG (Addgene # 34611), which we have described previously (11).

ShRNA sequences targeting HIF1α, HIF2α, or HIF1β/ARNT (**Table S3**) were obtained from the MISSION® TRC shRNA library (Sigma) or were previously described (12). Scramble shRNA sequence 1 was from the MISSION® TRC shRNA library while scramble shRNA sequence 2 (**Table S3**) has been previously reported (13). These sequences were sub-cloned into the lentivirus transfer plasmid pLKO.1 vector (Addgene # 8453).

Lentiviral infections. Stable cells were generated by lentivirus infection essentially as described by us previously (11, 14). Briefly, lentivirus was produced in HEK293T cells by co-

transfecting transfer plasmids described above with plasmids coding for a third generation packing system we routinely use (pRSV-Rev, pRRE, and pCMV-VSVG) (11, 14). Viral supernatants were collected 40-48 h post-transfection. HepG2 cells for infection were plated in a 60 mm dish 24 h before infection so that cells reached a confluence of 30% on the day of infection. Collected viral supernatants were filtered through a 0.45-μm polyvinylidene difluoride filter, and cells were incubated with a 1:2 dilution of viral supernatant containing 5 μg/mL Polybrene (Santa Cruz). Media was changed the next day to fresh MEM supplemented with 10% fetal bovine serum, penicillin (100 IU/ml), and streptomycin (100 μg/ml). Forty-eight hours after infection, for dominant negative and shRNA-infections, 2 μg/mL puromycin (Sigma-Aldrich) was added to obtain puromycin-resistant cells (the transfer plasmid for luciferase constructs did not confer resistance to puromycin). For HIF1α+HIF2α double knockdown, cells were sequentially infected with lentivirus targeting HIF1α and HIF2α, and the infections were spaced by one week. Control infection cells for the double knockdown were exposed to lentivirus containing scrambled shRNA followed one week later by lentivirus lacking a transfer plasmid.

Quantitative RT-PCR assays. RNA extraction from HepG2 cells and mouse tissue, reverse transcription to cDNA, and qRT-PCR analyses were performed as described by us previously (5, 15). Transcript levels were quantified using the $\Delta\Delta C_T$ method with *18S* (in mice) or *TBP* (in HepG2 cells) as the internal control, also as described by us previously (5, 15). Primers used are listed in **Table S4**.

Cell viability assays. These were performed using the 3-(4,5-dimethylthiazol-2-yl)-2,5-diphenyl tetrazolium bromide (MTT) reagent (Sigma) as described by us previously (5, 15).

Inductively coupled plasma mass spectrometry. Metal measurements using ICP-MS were performed exactly as described by us previously (5, 15-17).

Open-field assays for neurobehavior assessment. Open-field analyses were performed as described in our recent publication (17).

Immunofluorescence microscopy. This was also performed as described by us previously (5, 15, 17). Briefly, cells were grown on glass coverslips, fixed with 3% paraformaldehyde, and processed for staining as previously reported (5, 15, 17). Nucleus was stained using 4′,6-diamidino-2-phenylindole (DAPI). Imaging was using a Nikon swept field confocal equipped with a four-line high-power laser launch and 60X, 1.4 numerical aperture oil-immersion objective (Nikon). Image capture was with an iXon3 X3 DU897 EM-CCD camera (Andor Technology).

Immunoblots. HepG2 cells were cultured in 35 mm dishes, treated with or without Mn, MG132 and/or prolyl hydroxylase inhibitors, and scrapped using 200 μl of RIPA buffer (50 mM Tris-HCl, pH 7.4; 150 mM NaCl; 1 mM EDTA; 1% Triton; 0.25% sodium deoxycholate; protease inhibitors cocktail (Thermo A32953)). Whole-cell lysates were prepared by adding loading buffer (50 mM Tris-HCl, pH 7.4; 2% sodium dodecyl sulfate; 10% glycerol, 0.1 M dithiothreitol; 0.01% (weight/volume) bromophenol blue) and boiling the samples for 5 min. Equal volumes of samples were loaded per lane. Further processing was as described by us previously (15). Images were quantified using ImageQuant TL software (GE).

Luciferase assays. HepG2 cells stably expressing luciferase constructs were treated with or without 250 μM Mn for 16 h. Luciferase assays were performed using the Luciferase Assay System kit (Promega) according to the manufacturer's instruction and normalized to protein content (Bio-Rad protein assay dye, #5000006).

Transcription factor binding prediction. Transcription factors predicted to bind the *SLC30A10* promoter were identified using the PROMO-ALGGEN algorithm (18, 19).

Antibodies and chemicals. We used the following commercial primary antibodies in this study: rabbit polyclonal anti-HIF1α (Abcam, Ab2185), rabbit polyclonal anti-HIF2α (Novus, NB100-122), rabbit monoclonal anti-HIF1α proline 564 (Cell signaling, 3434S), and mouse monoclonal anti-tubulin (Sigma, T5168). We have previously described the custom rabbit polyclonal anti-SLC30A10 antibody raised against the C-terminus of human SLC30A10 that detects SLC30A10 in human cell lines (but not in mouse tissue) (5, 17). Sources of chemicals not provided elsewhere were Thermo Fisher Scientific or Sigma-Aldrich.

Statistical analyses. Cell culture experiments were replicated three or more times independently. Animal numbers are provided in the figure legends. Comparisons between multiple groups were performed using one- or two-way ANOVA and appropriate *post hoc* tests. Comparisons between two groups were performed using Student's *t*-test. The Prism 8 software (GraphPad, La Jolla, CA) was used. $P < 0.05$ was considered to be significant. Asterisks in graphs denote statistically significant differences.

Supplemental Figures

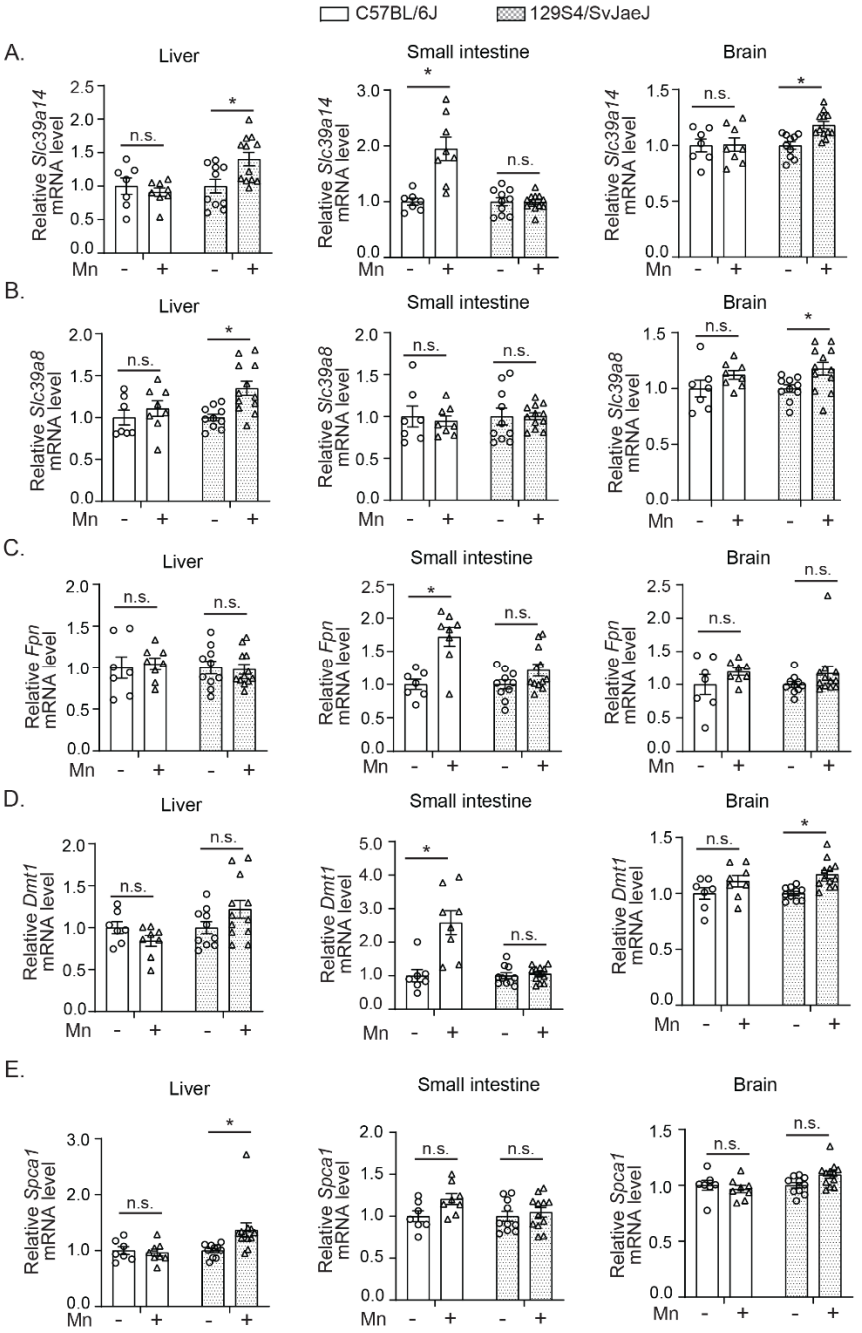

Fig.S1. Mn-induced changes in expression of Mn transporters in 129S4/SvJaeJ or C57BL/6J mice.

A-E. Samples analyzed for SLC30A10 expression in **Fig.1** were processed for analyses of transporters indicated above by qRT-PCR. Sample processing, animal number, and normalization were identical to **Fig.1**. Mean ± SE. *P<0.05 by two-way ANOVA (strain and Mn treatment as independent variables) and Sidak's *post hoc* test for indicated comparisons; n.s., not significant.

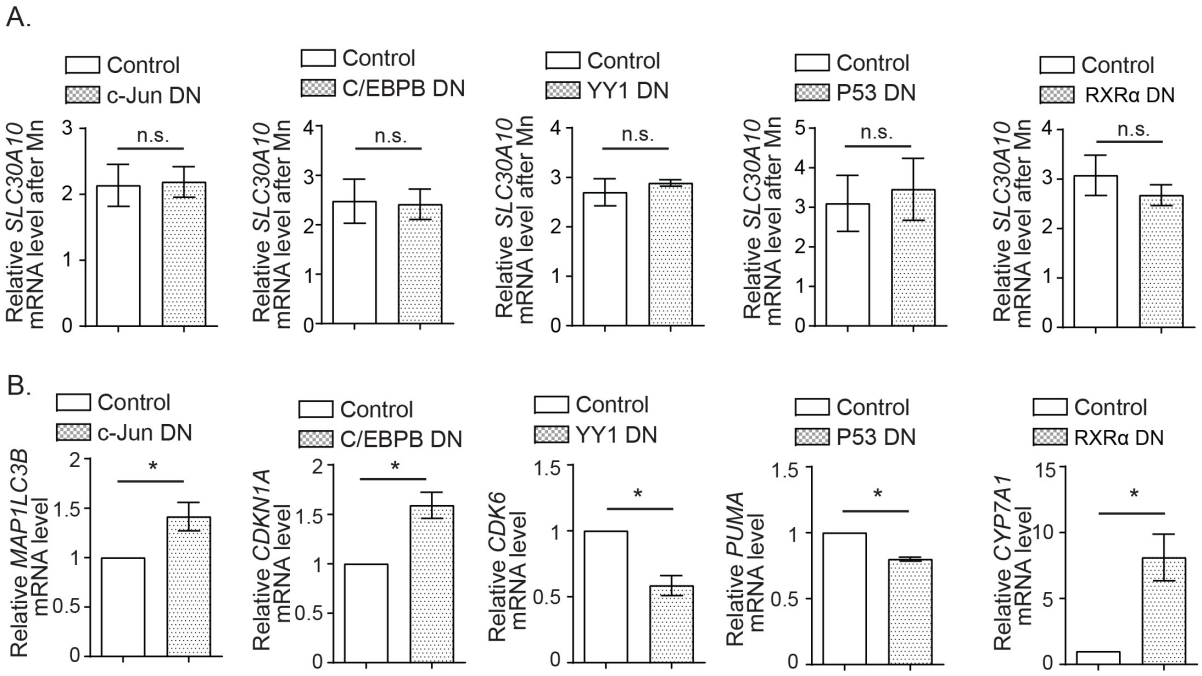

Fig.S2. c-Jun, C/EBPB, YY1, P53, and RXRα are not required for the Mn-induced increase in SLC30A10 expression.

A. qRT-PCR analyses in HepG2 cells stably expressing dominant negative (DN) versions of c-Jun, C/EBPB, YY1, P53, or RXRα, or infection control cells treated with 0 or 250 μM Mn for 4 h. Expression without Mn treatment was normalized to 1 for each infection condition. N=3-4. There were no differences between groups by *t*-test.

B. qRT-PCR analyses in HepG2 cells infected with indicated dominant negative mutants or infection control cells. Expression in infection control cells was normalized to 1. N=3. *P<0.05 by *t*-test.

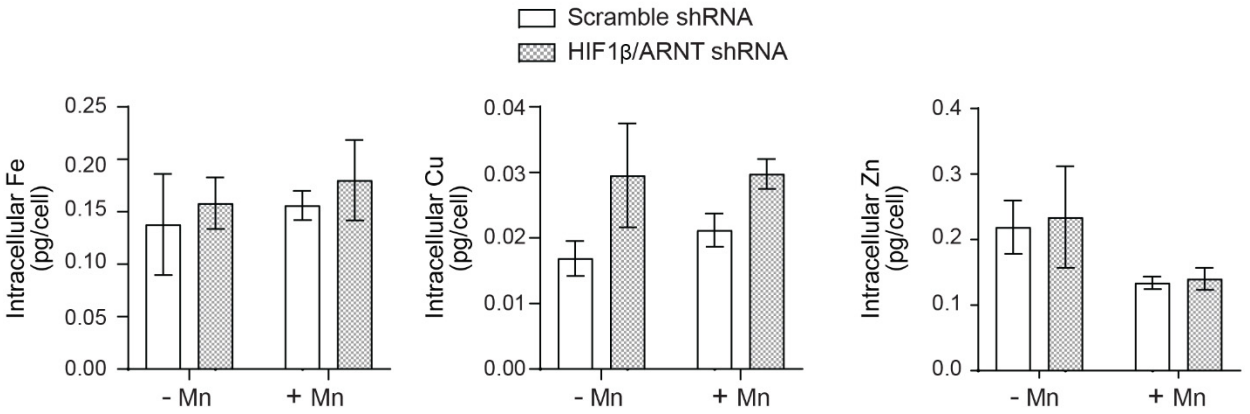

Fig.S3. Intracellular levels of Fe, Cu, and Zn are not affected by knockdown of HIF1β/ARNT.

Amounts of Fe, Cu, and Zn were quantified in samples used for Mn measurements in **Fig.7A**. Sample size is identical to **Fig.7A**. Data are mean ± SE. There were no differences between groups using two-way ANOVA.

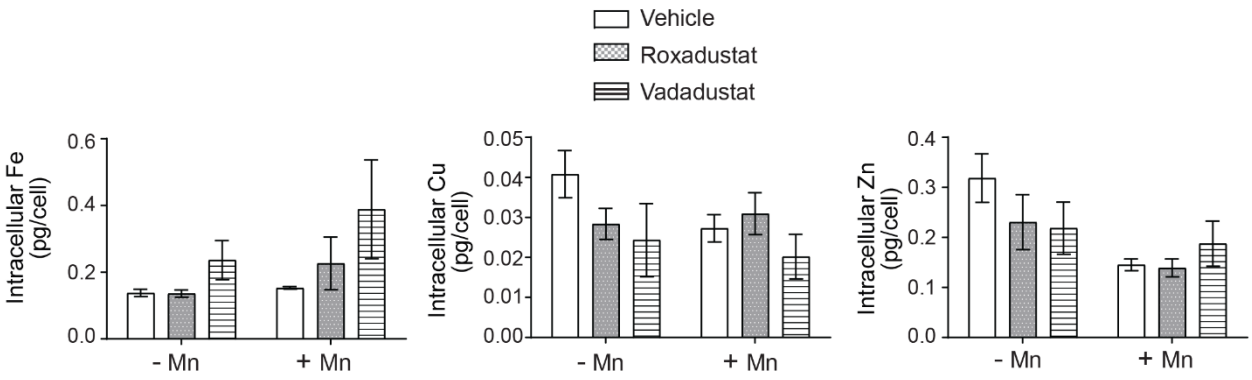

Fig.S4. Effect of roxadustat or vadadustat on intracellular Fe, Cu, and Zn.

Fe, Cu, and Zn levels were quantified in samples used for Mn measurements in **Fig.8D**. Sample size is identical to **Fig.8D**. Data are mean ± SE. Within cells that did or did not receive Mn, there was no effect of roxadustat or vadadustat treatment on Fe, Cu, or Zn levels by two-way ANOVA.

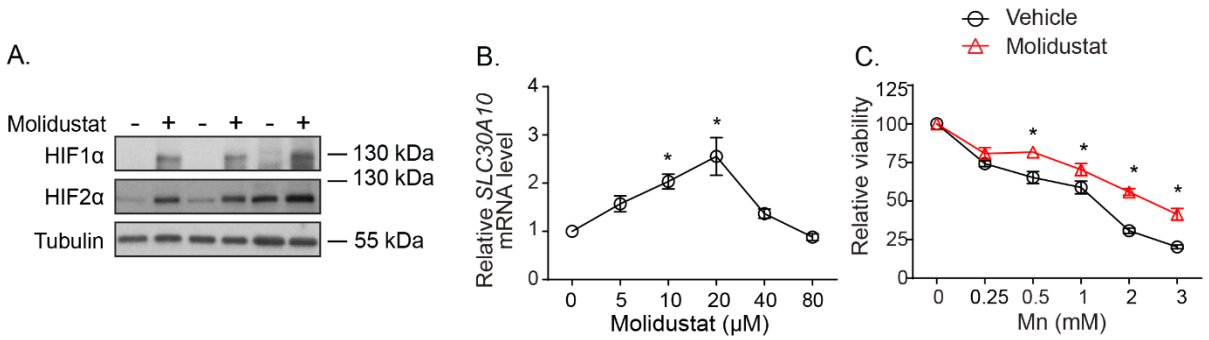

Fig.S5. Molidustat increases HIF1α and HIF2α protein as well as SLC30A10 expression, and protects against Mn-induced cell death.

A. Immunoblot analyses after treatment of HepG2 cells with 0 or 20 μM molidustat for 16 h.

B. qRT-PCR analyses after treatment of HepG2 cells with indicated levels of molidustat for 16 h. N=3. Mean ± SE. *P<0.05 by one-way ANOVA and Dunnett's *post hoc* test for comparison between no drug and other conditions.

C. Cell viability assays in HepG2 cells after treatment with or without 20 μM molidustat for 16 h followed by exposure to indicated levels of Mn for 24 h. Viability of cells treated with or without molidustat in the absence of Mn exposure were separately normalized to 100. N=4. Mean ± SE. *P<0.05 by two-way ANOVA (drug and Mn treatment as independent variables) and Sidak's *post hoc* test for comparisons between treatment conditions at each Mn dose.

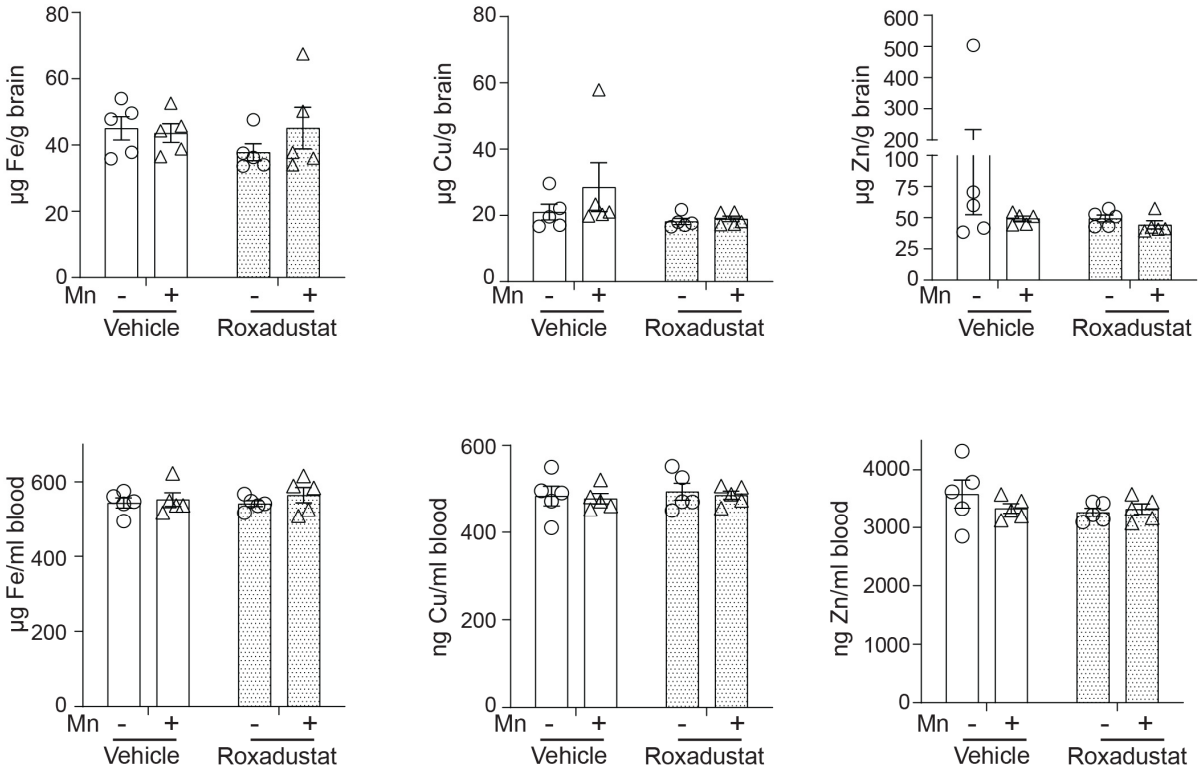

Fig.S6. Effect of roxadustat on blood and brain Fe, Cu, and Zn levels.

Fe, Cu, and Zn levels were quantified in tissue samples used for Mn measurements in **Fig.10C**. Sample size is identical to **Fig.10C**. Data are mean ± SE. There was no effect of roxadustat on Fe, Cu, or Zn levels in blood or brain by two-way ANOVA.

Supplemental Tables

Transcript	Relative expression after Mn	*t*-test in comparison with vehicle
SLC30A10	2.40 ± 0.28	p<0.05
SLC39A14	0.71 ± 0.02	p<0.05
SLC39A8	0.87 ± 0.09	n.s.
SPCA1	1.00 ± 0.05	n.s.
FPN	0.77 ± 0.21	n.s.
DMT1	0.92 ± 0.03	p<0.05
VEGF	2.41 ± 0.29	p<0.05

Table S1. Mn upregulates SLC30A10 and VEGF expression in HepG2 cells.

Cells were treated with 0 or 250 μM Mn for 4 h, and gene expression was analyzed by qRT-PCR. For each transcript, expression without Mn treatment was normalized to 1. N=4. Data are mean ± SE. N.S. – not significant.

shRNA	Transcript	Relative expression in comparison with scramble shRNA	*t*-test or ANOVA in comparison with scramble shRNA
HIF1α	*HIF1α*	0.16±0.02	p<0.05
HIF1α	*HIF2α*	1.13± 0.13	n.s.
HIF2α	*HIF1α*	1.42 ± 0.11	p<0.05
HIF2α	*HIF2α*	0.29 ± 0.07	p<0.05
HIF1β/ARNT sequence 1	*HIF1β/ARNT*	0.59±0.03	p<0.05
HIF1β/ARNT sequence 2	*HIF1β/ARNT*	0.47±0.02	p<0.05
HIF1α + HIF2α	*HIF1α*	0.20±0.01	p<0.05
HIF1α + HIF2α	*HIF2α*	0.35±0.02	p<0.05

Table S2. Validation of shRNAs targeting HIF1α, HIF2α or HIF1β/ARNT.

qRT-PCR analyses in HepG2 cells stably infected with scramble shRNAs or shRNAs targeting HIF1α, HIF2α, HIF1β/ARNT or HIF1α + HIF2α. Expression in respective scramble shRNA control cells was normalized to 1. Scramble shRNA sequence 1 was used for the HIF1α shRNA assay (single knockdown). Scramble shRNA sequence 2 was used for the other experiments, including HIF1α + HIF2α double knockdown. N=3-4. Except HIF1β/ARNT shRNAs, $p<0.05$ by *t*-test in comparison with respective scramble shRNA. For HIF1β/ARNT shRNAs, $p<0.05$ by one-way ANOVA and Dunnett's *post hoc* test in comparison with scramble shRNA. N.S. – not significant.

shRNA	Sequence	Reference
HIF1α	TGCTCTTTGTGGTTGGATCTA	(12)
HIF2α	CAGTACCCAGACGGATTTCAA	TRCN0000003806(MISSION® shRNA library (Sigma))
HIF1β shRNA-1	AGCCTCATCATCGTTCAAGTT	TRCN0000003820(MISSION® shRNA library (Sigma))
HIF1β shRNA-2	GCCTACACTCTCCAACACAAT	TRCN0000003816(MISSION® shRNA library (Sigma))
Scramble shRNA-1	CAACAAGATGAAGAGCACCAA	SHC002(MISSION® shRNA library (Sigma))
Scramble shRNA-2	GTGGACTCTTGAAAGTACTAT	(13)

Table S3. Sequences of shRNAs used. For HIF1β/ARNT and scramble shRNAs, the numbers 1 and 2 refer to sequence 1 and 2.

Gene	Species	Forward primer sequence	Reverse primer sequence
HIF1α	Human	CCACAGGACAGTACAGGATG	TCAAGTCGTGCTGAATAATACC
HIF2α	Human	GCGACAATGACAGCTGACAA	CAGCATCCCGGGACTTCT
HIF1β	Human	CTAGTGGCCATTGGCAGATT	CAATGTTGTGTCGGGAGATG
SLC39A8	Human	ATGCTACCCAAATAACCAGC	CAGGAATCCATATCCCCAAAC
DMT1	Human	TGGCTTATCTGGGCTTTGTG	CACACTGGCTCTGATGGCTA
SLC39A14	Human	TGTCTCCAAGTCTGCAGTGG	GGAATCATGTGGTCCAGGTC
SLC30A10	Human	TTCCCGCTTATCAAGGAGACC	ACTGCTAATTCCAGGCACAGC
FPN	Human	CAGTTAACCAACATCTTAGC	AAGCTCATGGATGTTAGAG
SPCA1	Human	GGATAGAGTTCCTGCTGACTTAC	TGAGGAGCTGTCACCTTAGA
VEGF	Human	GGGTCTCGATTGGATGGCA	AGGGCAGAATCATCACGAAGT
MAP1LC3B	Human	CCGCCGCCTTTTTGGGTAG	GAGTCAGGGACCTTCAGCAG
CDK6	Human	CGCCTATGGGAAGGTGTTC	TTGGGGTGCTCGAAGGTCT
CDKN1A	Human	ACCTGGAGACTCTCAGGGTCG	TTAGGGCTTCCTCTTGGAGAAGAT
PUMA	Human	CTGTGAATCCTGTGCTCTGC	AATGAATGCCAGTGGTCACA
CYP7A1	Human	CCATAAGGTGTTGTGCCACG	CATCCATCGGGTCAATGCTT
TBP	Human	CGAACCACGGCACTGATTTTC	TTTCTTGCTGCCAGTCTGGAC
Slc39a14	Mouse	AAGTCCCTGCTCGACCAC	CTGGGAATCCAGCTGCTG
Slc39a8	Mouse	CTCGCCTTCAGTGAGGATGT	GCTTTGCGTTGTGCTTTCTT
Dmt1	Mouse	TCAGAGCTCCACCATGACTG	TGTGAACGTGAGGATGGGTA
Slc30a10	Mouse	GTAGCAGGTGATTCCCTGAAC	GTGATGACCACAACCACGGAC
Fpn	Mouse	TTGCAGGAGTCATTGCTGCTA	TGGAGTTCTGCACACCATTGAT
Spca1	Mouse	GACTCTAGCCCTTGGTGTTATG	CTTCGTCAGGGTTCCAGTTT
18S	Mouse	CATTAAGGGCGTGGGGCGG	GTCGTGGGTTCTGCATGATG

Table S4. qRT-PCR primers.

Supplemental References

1. Taylor CA*, et al.* (2020) Maintaining Translational Relevance in Animal Models of Manganese Neurotoxicity. *J Nutr* 150(6):1360-1369.
2. Felber DM, Wu Y, & Zhao N (2019) Regulation of the Metal Transporters ZIP14 and ZnT10 by Manganese Intake in Mice. *Nutrients* 11(9):2099.
3. Mercadante CJ*, et al.* (2019) Manganese transporter Slc30a10 controls physiological manganese excretion and toxicity. *J Clin Invest* 129(12):5442-5461.
4. Bouchard MF*, et al.* (2011) Intellectual impairment in school-age children exposed to manganese from drinking water. *Environ Health Perspect* 119(1):138-143.
5. Liu C*, et al.* (2017) Hypothyroidism induced by loss of the manganese efflux transporter SLC30A10 may be explained by reduced thyroxine production. *J Biol Chem* 292(40):16605-16615.
6. Lee K*, et al.* (2010) LW6, a novel HIF-1 inhibitor, promotes proteasomal degradation of HIF-1alpha via upregulation of VHL in a colon cancer cell line. *Biochem Pharmacol* 80(7):982-989.
7. Bensaude O (2011) Inhibiting eukaryotic transcription: Which compound to choose? How to evaluate its activity? *Transcription* 2(3):103-108.
8. Coneyworth LJ*, et al.* (2012) Identification of the human zinc transcriptional regulatory element (ZTRE): a palindromic protein-binding DNA sequence responsible for zinc-induced transcriptional repression. *J Biol Chem* 287(43):36567-36581.
9. Schulman IG, Juguilon H, & Evans RM (1996) Activation and repression by nuclear hormone receptors: hormone modulates an equilibrium between active and repressive states. *Molecular and Cellular Biology* 16(7):3807-3813.
10. Qiao H & May JM (2012) Interaction of the transcription start site core region and transcription factor YY1 determine ascorbate transporter SVCT2 exon 1a promoter activity. *PloS one* 7(4):e35746.
11. Zogzas CE & Mukhopadhyay S (2018) Putative metal binding site in the transmembrane domain of the manganese transporter SLC30A10 is different from that of related zinc transporters. *Metallomics* 10(8):1053-1064.
12. Briggs KJ*, et al.* (2016) Paracrine Induction of HIF by Glutamate in Breast Cancer: EglN1 Senses Cysteine. *Cell* 166(1):126-139.
13. Wiederschain D*, et al.* (2009) Single-vector inducible lentiviral RNAi system for oncology target validation. *Cell Cycle* 8(3):498-504.
14. Selyunin AS, Iles LR, Bartholomeusz G, & Mukhopadhyay S (2017) Genome-wide siRNA screen identifies UNC50 as a regulator of Shiga toxin 2 trafficking. *J Cell Biol* 216(10):3249-3262.
15. Leyva-Illades D*, et al.* (2014) SLC30A10 Is a Cell Surface-Localized Manganese Efflux Transporter, and Parkinsonism-Causing Mutations Block Its Intracellular Trafficking and Efflux Activity. *J Neurosci* 34(42):14079-14095.
16. Hutchens S*, et al.* (2017) Deficiency in the manganese efflux transporter SLC30A10 induces severe hypothyroidism in mice. *J Biol Chem* 292(23):9760-9773.
17. Taylor CA*, et al.* (2019) SLC30A10 transporter in the digestive system regulates brain manganese under basal conditions while brain SLC30A10 protects against neurotoxicity. *J Biol Chem* 294(6):1860-1876.
18. Farre D*, et al.* (2003) Identification of patterns in biological sequences at the ALGGEN server: PROMO and MALGEN. *Nucleic Acids Res* 31(13):3651-3653.
19. Messeguer X*, et al.* (2002) PROMO: detection of known transcription regulatory elements using species-tailored searches. *Bioinformatics* 18(2):333-334.